


Article

Polychromy in Ancient Greek Sculpture: New Scientific Research on an Attic Funerary Stele at the Metropolitan Museum of Art

Elena Basso ^{1,*} , Federico Carò ¹ and Dorothy H. Abramitis ²

¹ Department of Scientific Research, The Metropolitan Museum of Art, 1000 Fifth Avenue, New York, NY 10028, USA

² Department of Objects Conservation, The Metropolitan Museum of Art, 1000 Fifth Avenue, New York, NY 10028, USA

* Correspondence: elena.basso@metmuseum.org; Tel.: +1-212-731-1098

Abstract: Polychromy in Ancient Greek Sculpture was the subject of the exhibition *Chroma: Ancient Greek Sculpture in Color*, held at The Metropolitan Museum of Art (The Met), New York, in 2022–2023. On this occasion, a multidisciplinary project involving The Met’s Departments of Greek and Roman Art, Objects Conservation, Imaging, Scientific Research, and colleagues from the Liebieghaus Polychromy Research Project in Frankfurt, Germany, was carried out to study an Attic funerary monument. The color decoration of the sphinx was reconstructed by combining non-invasive and minimally invasive techniques that provided information about surviving and lost pigments, original design, and painting technique. Results of multiband imaging, digital microscopy, and X-ray fluorescence spectroscopy guided the removal of minute samples from selected areas for examination by Raman spectroscopy and scanning electron microscopy, coupled with energy-dispersive X-ray spectroscopy, to shed light on the pigments and paint stratigraphy. The color palette included two varieties of blue, Egyptian blue and azurite, a carbon-based black pigment, two reds, cinnabar and red ocher, and yellow ocher, all painted directly over the marble without a preparation layer. The scientific findings informed the physical reconstruction of the sphinx made by archaeologists from the Liebieghaus Polychromy Research Project, featured in the exhibition.

Keywords: polychromy; Egyptian blue; non-invasive analysis; multiband imaging; XRF; microscopy; SEM-EDS; Raman



Citation: Basso, E.; Carò, F.; Abramitis, D.H. Polychromy in Ancient Greek Sculpture: New Scientific Research on an Attic Funerary Stele at the Metropolitan Museum of Art. *Appl. Sci.* **2023**, *13*, 3102. <https://doi.org/10.3390/app13053102>

Academic Editors: Daniela Di Martino, Maria Pia Riccardi and Massimiliano Clemenza

Received: 3 February 2023
Revised: 25 February 2023
Accepted: 25 February 2023
Published: 28 February 2023



Copyright: © 2023 by the authors. Licensee MDPI, Basel, Switzerland. This article is an open access article distributed under the terms and conditions of the Creative Commons Attribution (CC BY) license (<https://creativecommons.org/licenses/by/4.0/>).

1. Introduction

The polychromy of ancient Greek sculptures has been the subject of studies for over a century, as remains of painted decorations were already documented during the archaeological excavation of the Athenian Acropolis at the end of 19th century [1]. Watercolor illustrations of colored sculptures and architectural elements were painted immediately after their discovery, in an attempt to “photograph” their ephemeral appearance due to the acceleration of degradation processes. Polychromy was extensively used on stone sculptures [2–4], architectural elements [5,6], and on terracotta figurines [7–9] as a constituent component of three-dimensional artworks due to the symbolic, communicative, and aesthetic use of color [10]. After the Second World War, the debate about the polychromy of ancient sculptures attracted scholars from many disciplines, whose research has been devoted to the reconstruction of the original appearance of artefacts through investigation of their surfaces and the analysis of pigment remains since then [3,11–26]. Advances in technical photography strongly enhanced out capacity to visualize residual traces of pigments, becoming crucial in creating three-dimensional, physical reconstructions of painted sculptures [1,12,13].

The Metropolitan Museum of Art (The Met) has been part of the conversation about ancient polychromy since the beginning of the 20th century, when Edward Robinson,

a Classical scholar author of an influential article on the subject in 1892, encouraged the acquisition of sculptures showing residual paint traces, to convey insight into their original appearance, during his tenure as The Met's director [27]. Renowned classical archaeologist and former Met curator Gisela M. A. Richter made significant contributions to the field through careful analyses of many works in the collection [28,29]. The Met contributed to the ongoing conversation about polychromy with the exhibition *Chroma: Ancient Sculpture in Color*, opened in July 2022. During the exhibition preparation, an ambitious multidisciplinary project was initiated to investigate the extant and original polychromy of ancient sculptures within the Museum's Greek and Roman collections. Several museum departments were involved in the project, including Greek and Roman Art, Objects Conservation, Imaging, and Scientific Research. Among the several studied sculptures, an Attic funerary stele carved from Parian marble, which features a youth and a young girl, its capital and finial in the form of a sphinx (11.185a–d, f, g, x, Figure 1), received special attention, not only because it is one of the most extensively painted monuments in the Greek and Roman collections, but also because the exhibition included a reconstruction of the sphinx finial realized by Vinzenz Brinkmann, Head of the Department of Antiquities at the Liebieghaus Skulpturensammlung in Frankfurt, and Ulrike Koch-Brinkmann.

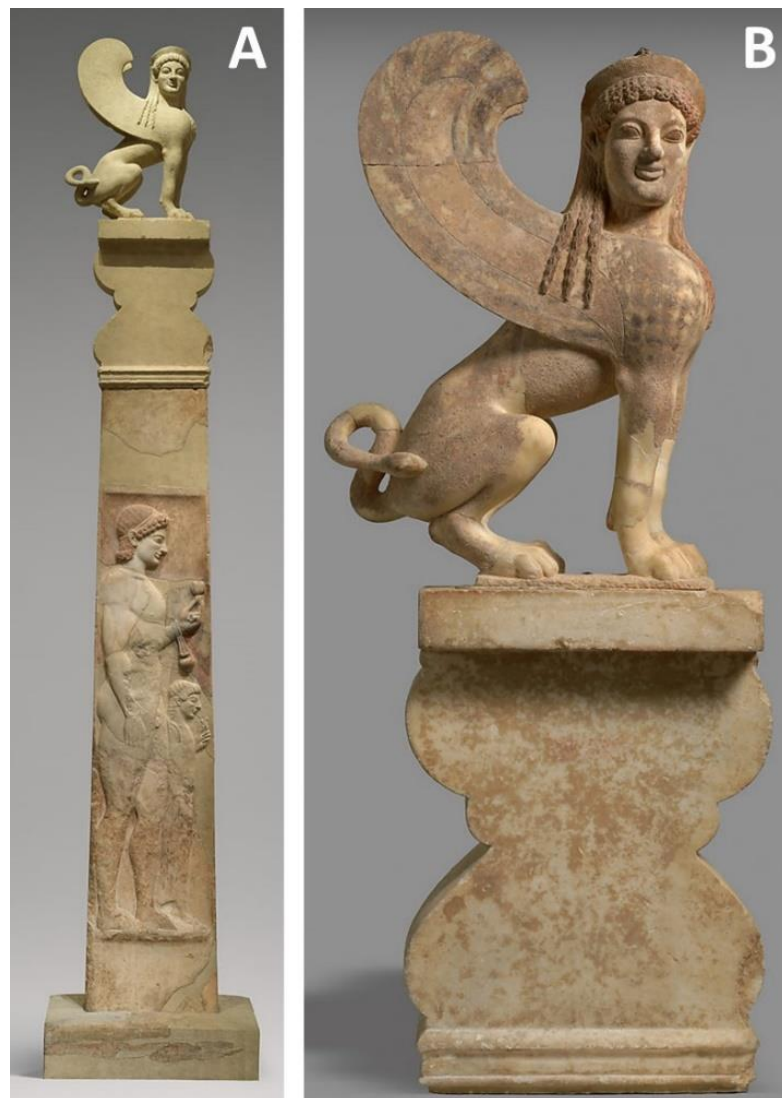


Figure 1. Marble stele with a youth and little girl, and a capital and finial in the form of a sphinx (11.185a–d, f, g, x). (A) Overall view; (B) Marble capital and sphinx. Greek, Attic, ca. 530 BCE. The Metropolitan Museum of Art, New York.

This unique funerary monument, extensively described in [30], is more than 4 m high (about 14 feet) and is displayed in two separate set ups: the stele on one side, and the sphinx with its capital in a display case next to the stele (Figure 1). Traces of original color were documented in previous studies [28,29] based on visual observation, but not supported by scientific analyses. With the main goal of understanding the paint materials and uses on funerary monuments, the identification and distribution of pigments was achieved using a suite of non-invasive and micro-invasive scientific techniques. The technical and scientific investigation of the Attic grave stele presented analytical challenges that well exemplify the constraints often encountered when working on objects belonging to museum collections. First and foremost, the sphinx finial, carved in the round, could not be removed from the display case in the gallery, nor could the case be dismantled, allowing access only to the front and part of the sides of the sculpture. Moreover, the number of representative samples and their sizes had to be greatly minimized to comply to the most recent standards of museum's practices, which reduce irreversible interventions on works of art.

As a result of such technical constraints, the analytical protocol designed to investigate the polychromy of the grave stele relied heavily on non-invasive techniques by working directly on the sculpture in the gallery. The intrinsic limitations of non-invasive techniques drove the research towards a micro-invasive approach, which had the potential to provide more comprehensive data. Micro-samples were removed when strictly necessary, specifically to investigate the stratigraphy of the paint layers from areas of the sculpture where it appeared preserved, and to complement non-invasive analysis in case of unclear results.

Despite the challenges, the adopted methodology contributed to our knowledge of the painters' techniques, the original decorative scheme, and the pigments present on the sculpture's surfaces, highlighting the role of science and scholarship in identifying and interpreting surface treatments on ancient artworks. Results were featured in the exhibition narrative and incorporated into an augmented reality experience, allowing visitors to elevate their observation and understanding of artworks.

2. Experimental

The initial assessment was undertaken using multiband imaging (MBI), particularly helpful in gaining a broad overview of an object in a relatively short amount of time. The suite of images was useful in determining the presence of materials not visible to the unaided eye, often through the appearance of a characteristic luminescence, or by a difference in color. These images were stacked using the commercial software Adobe Photoshop to determine the precise location of a finding. The MBI findings were supplemented with microscopy, which provided information about the surviving pigments and the original chromatic scheme. These data were used to guide several campaigns of complementary non-invasive analyses, including portable X-ray fluorescence spectroscopy (pXRF) and scanning X-ray fluorescence spectroscopy (sXRF), which were followed by the collection of ten representative micro-samples with the aid of a binocular microscope and surgical scalpel. Most of the samples were obtained in the form of loose particles by mechanical scraping, while two samples collected from the sphinx's hair included the marble substrate, the paint and accretion layers.

The samples were studied using polarized light microscopy (PLM), scanning electron microscopy (SEM), energy dispersive spectroscopy (EDS), micro-Raman spectroscopy, and micro-X-ray diffraction (μ XRD). The fragments that included a complete stratigraphy were embedded in Buehler Epothin[®] epoxy resin, cross-sectioned, and polished using Micromesh[®] cloths, followed by ion milling by means of a Hitachi IM4000 ion milling system.

2.1. Multiband Imaging

Multiband imaging was carried out using a modified Canon D60 camera (IR/UV filters removed) (Canon USA Inc., Melville, NY, USA), with a Coastal Opt UV-Vis-IR 60 mm macro lens (The Jenoptik AG, Jena, Germany). The following lens filters were used:

IDAS-UIBAR (ICAS Enterprises, Tokyo, Japan) for visible (VIS); IDAS-UIBAR + a Kodak 2E Wratten (Eastman Kodak Company, Rochester, NY, USA) or IDAS-UIBAR + Schott 418 filter (Schott Company, Mainz, Germany) for ultraviolet-induced visible luminescence (UVL); X-Nite BP1 + X-Nite 330 filter for ultraviolet-reflectance (UVR); X-Nite 830 filter for infrared-reflectance (IRR) and visible-induced infrared luminescence (VIL) (All X-Nite filters: Llewellyn Data Processing (LDP LLC), Carlstadt, NJ, USA). UVR, IRR, and VIL monochrome images were created in Adobe Camera RAW with the black and white function. False color (FC) images were generated in Adobe Photoshop (PS) (Adobe Inc., San Jose, CA, USA). A pair of three-channel (UV-VIS-IR) LED fixtures were used for illumination. VIS source: 5000k with 99CRI/RA, ISO 3664:2009 (viewing booth quality), approx. 1500 Lumens (per fixture) and approx. 17W. IR source: peak output at 940 nm and approx. 19 W (per fixture). UV source: peak output at 365 nm and 18W (per fixture). A pair of red LED strip lights (peak output of 630 nm; 640 lumens per 4' fixture, 18WL) were used for VIL.

Since the sphinx could not be moved from the gallery, a mobile dark room was built around the sculpture to block out ambient light using sheets of black foam core board, taped together to create four sides and a ceiling (Supplementary Materials: Figure S1). The interior was large enough to accommodate lights and a camera on a tripod, yet the structure was easily dismantled for reuse.

2.2. Digital Microscopy

Digital microscopy images were taken in situ using a Keyence VHX-6000 digital microscope with a VH-ZST dual objective 20–200x zoom lens (Keyence Corporation, Itasca, IL, USA) mounted on a tripod.

2.3. XRF

Point XRF measurements were collected with a Bruker Tracer III-SD using Ti/Al/Cu filtered Rh radiation at 40 kV, 30 μ A for 60 s of live-time acquisition.

Scanning XRF was performed using a Bruker Elio XGLab energy-dispersive portable XRF spectrometer (Bruker Nano GmbH, Berlin, Germany) with a high-resolution large-area silicon drift detector (SDD) with 130 eV at manganese (Mn) $K\alpha$ with 10 kcps input photon rate (high resolution mode), and 170 eV at Mn $K\alpha$ with 200 kcps input photon rate (fast mode). The system was equipped with changeable filters and a rhodium (Rh) transmission target with 50 kV maximum voltage and 4 W maximum power. Elemental 2D mapping of the surface was achieved through automatic XY raster scanning. The translator stage can cover a maximum area of 10 \times 10 cm with an accuracy of 10 μ m. Parameters employed for the scans were 40 kV voltage, 80 μ A current, a dwell time of 1 s, and a step size of 1 mm. Elemental maps were then processed using the Fundamental Parameters software package PyMCA [31].

2.4. Raman Spectroscopy

Micro-invasive analysis was performed on select samples using a Bruker Senterra Raman spectrometer (Bruker Optics GmbH, Ettlingen, Germany) equipped with an Olympus 50x long-working-distance microscope objective and a charge-coupled device (CCD) detector. A Spectra Physics Cyan solid-state laser and continuous wave diode laser emitting at 488 and 785 nm, respectively, were used as the excitation sources, and two holographic gratings (1800 and 1200 rulings/mm) provided a spectral resolution of 3–5 cm^{-1} . The output laser power, number of scans, and integration times were adjusted according to the Raman response of the different samples.

Spectra were interpreted by comparison with The Met in-house database, and with the published literature.

2.5. SEM-EDS

Analyses of carbon-coated samples were performed with a FE-SEM Zeiss Sigma HD (Zeiss Microscopy, Jena, Germany), equipped with an Oxford Instrument X-MaxN 80 SDD detector. Backscattered electron (BSE) images and energy-dispersive spectrometry (EDS) analyses were carried out with an accelerating voltage of 20 kV in high vacuum.

2.6. μ XRD

Micro-diffraction was performed with a Bruker D8 Advance (Bruker Optics GmbH, Ettlingen, Germany) using Cu K α radiation at 40 kV and 40 mA, equipped with a Göbel mirror, a 1 mm UBC collimator, and an Eiger2R 500k Hybrid Photon Counting detector working in 2D mode. Continuous scans were collected between 20° and 70°, with a step size of 0.02° and a time step of 1 s. Micro-samples were mounted on a rotating low-background plate.

3. Results

3.1. The Polychromy Scheme

The stele and the sphinx finial retain noticeable traces of the ancient polychromy, although the distribution and appearance of pigments have been affected by centuries of interaction with the atmosphere and the burial environment, as well as by its post-excavation history, especially on the front of the sculpture. On the shaft, red pigmentation is clearly visible in the background, on the youth's hair, and on the inscription carved on the rectangular base. Conversely, the front of the capital retains little visible pigment, except for a thin red line along the abacus edges and traces of red between the upper volutes. The detailed original painted decoration can only be seen on its front side by means of the PS-enhanced UVL, and, partially, by raking light imaging (Figure 2). Raking light images highlight the incised lines that were likely used to lay out the ornament on the capital (Figure 2B).

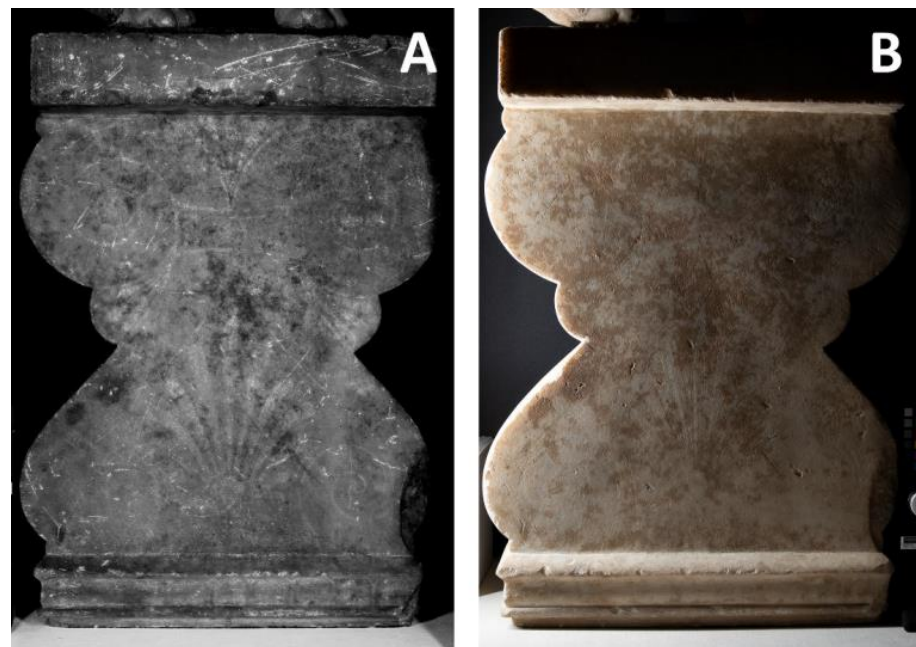


Figure 2. Images of the capital showing the intricate original decoration: (A) PS-enhanced UVL; (B) raking light.

The sphinx is the section with the most abundant preserved polychromy, particularly on the front. Red, blue, and black pigment remains, in different states of preservation, are visible in several areas of the marble surface, notably its chest, wing (Figure 3A), hair,

crown, and eyes. The most striking MBI finding on the sphinx appeared in the VIL image (Figure 3B). Bands of luminescence, characteristic of the pigment Egyptian blue, were visible on the wing. Initially thought to be in the areas of the blue pigment visible with the naked eye, the stacking of VIL and VIS images (Supplementary Materials: Figure S3) clearly showed that the luminescence occurred between the visible blue areas, in the sections previously thought to be unpainted.

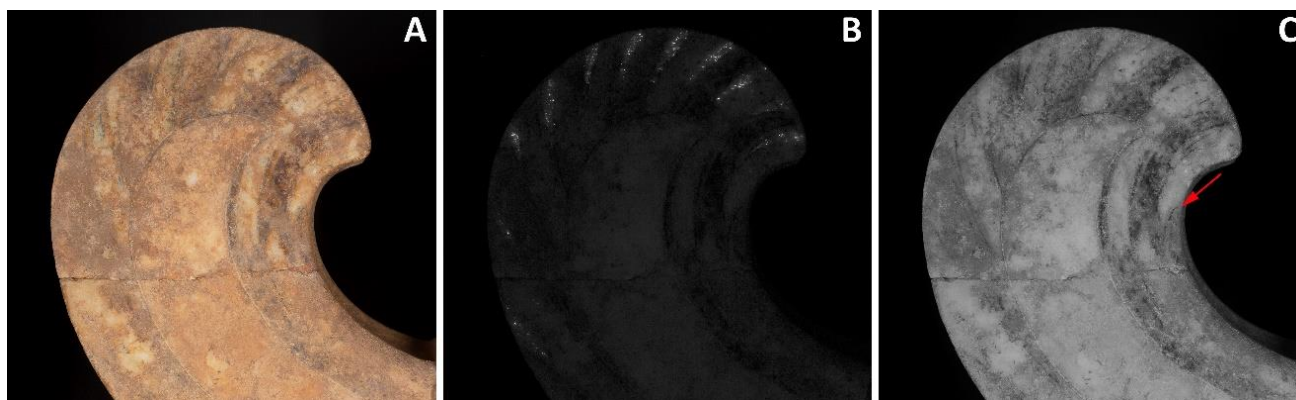


Figure 3. Imaging of the proper right wing of the sphinx: (A) VIS image showing traces of the original colors of the feathers; (B) VIL image illustrating the presence and distribution of the luminescence of Egyptian blue between the feathers; (C) IRR image highlighting the presence of black outlines defining the feathers, indicated by the red arrow.

The UVL images of the sphinx highlighted areas that were consolidated as part of past treatments (Supplementary Materials: Figure S2), while, as noted above, UVL of the capital provided details of the highly decorated front (Figure 2A).

Remains of blue color were documented by digital microscopy, whose high resolution and high magnification allowed the imaging of pigment remains, even when present as few discrete particles and in recessed areas (Supplementary Materials: Figure S4) such as the crown and the lines that separate the breast feathers from the leonine body.

The identification of pigments and the mapping of their distribution were obtained by combining imaging techniques with scientific analyses.

Results of multiband imaging and digital microscopy guided the first XRF analysis campaign that was performed in situ on areas with visible traces of pigments and where VIL indicated the presence of vestiges of Egyptian blue. Analyzed areas include: the shaft's background, the youth's hair and aryballos, the sphinx's wing, chest, head and hair, diadem, legs, and tail end, as well as the capital. Overall, XRF point measurements were characterized by the presence of dominant X-ray lines of calcium (Ca) and strontium (Sr) from the marble, and by lines of sulfur (S), titanium (Ti), manganese (Mn), iron (Fe), and lead (Pb), of variable intensity. In some areas, strong characteristic X-ray lines of copper (Cu) and mercury (Hg) were also detected, indicating the presence of Cu-based and Hg-based pigments.

In particular, Cu was detected in the wing, diadem, chest, and tail end, in areas where remains of blue pigment were still discernible. In the wing, the detection of Cu in sections that were luminescent in VIL images confirmed the presence of Egyptian blue. The second, undetermined blue pigment, already observed in MBI in the feathers, showed very intense signals of copper, the significant presence of which suggests another Cu-based blue pigment, likely azurite. The representative XRF spectra of dark red to black areas on the wing feathers and chest showed prominent X-ray lines of Hg, alongside intense X-ray lines of S, indicating the presence of cinnabar (HgS). The diffuse red color on the hair of the sphinx was characterized by a different XRF spectrum which included intense X-ray lines of Fe, accompanied by less intense lines of Mn, elements that are associated with red-brown ochres.

The detection of well-resolved, intense X-ray energy lines of Hg, associated with weak lines of S, by pXRF on darkened areas revealed the consistent presence of mercury sulfide, most likely a combination of cinnabar and metacinnabar (β -HgS) [32–37].

An XRF line scan recorded across the proper left eye showed variation in intensities of Hg and Fe X-ray lines, suggesting that cinnabar was used either in purity or mixed with ochre to represent the iris, and possibly the pupil (Supplementary Materials: Figure S5).

An Fe-based pigment containing traces of Mn, likely a red ochre, was also identified on the inscribed letters of the base and the shaft background, the youth's eye and hair, the sphinx's hair, carpal pad (Richter's pisiform bone), and in the areas between the wings and the tail's curl by pXRF analysis. In other locations, such as the sphinx's face, the leonine body, and the wings, the Fe-based pigments were either hindered by a thick crust resulting from burial or so scarce that their identification was not possible by means of non-invasive techniques. Digital microscopy proved essential in locating Fe-based pigment particles in highly disturbed surfaces, such as the sphinx's lips (Supplementary Materials: Figure S4C), where residual traces of the pigment were found deep in the groove that defines the lips. First observations by digital microscopy suggested that all the pigments were applied directly to the marble substrate.

Based on the combination of multiband imaging and XRF analysis, two types of Cu-based blue pigments were identified, as well as at least two types of red pigments, Fe- and Hg-containing, respectively. The presence of yellow, black, and white pigments was also inferred from observation of the surface at high magnifications.

In an attempt to define the original color scheme and inform reconstruction of the sphinx, elemental maps were collected by sXRF on selected areas of the sphinx's diadem, wing, and chest, and the capital (Figure 4).

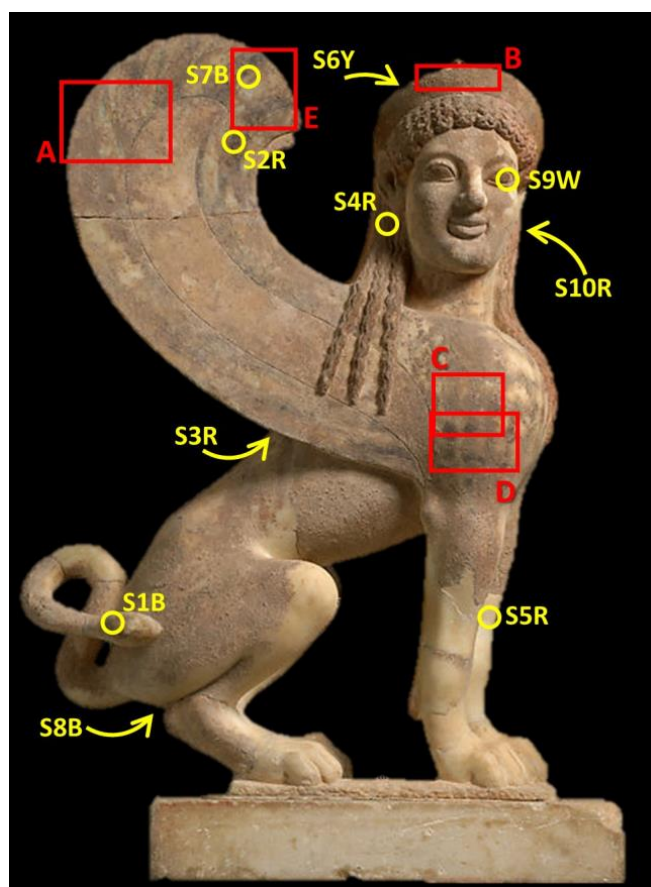


Figure 4. Locations of XRF maps and micro-samples. The arrows indicate sampling locations that are not visible in this frontal image.

Although currently completely concealed by a thick crust, glimpses of the original decoration of the diadem could be seen by shining a strong light through the marble (Supplementary Materials: Figure S6). Scanning XRF in this area helped identify the chromatic scheme of the decoration, by associating characteristic elements with specific pigments. The distribution of Hg, Cu, and Fe on the analyzed area of the diadem (Figure 4, area B, and Figure 5) reproduces the geometric design; in particular, Hg and Cu clearly identify the design of repeating red and blue meanders. The presence of Hg is indicative of cinnabar, whereas Cu suggests the use of a Cu-based pigment, possibly azurite, as the absence of luminescence in VIL images excludes the presence of Egyptian blue. Although the distribution of Fe might be indicative of the presence of Fe-containing pigments, mostly ochres, its identification is complicated by the abundance of iron oxides/hydroxides in accretions and patinas.

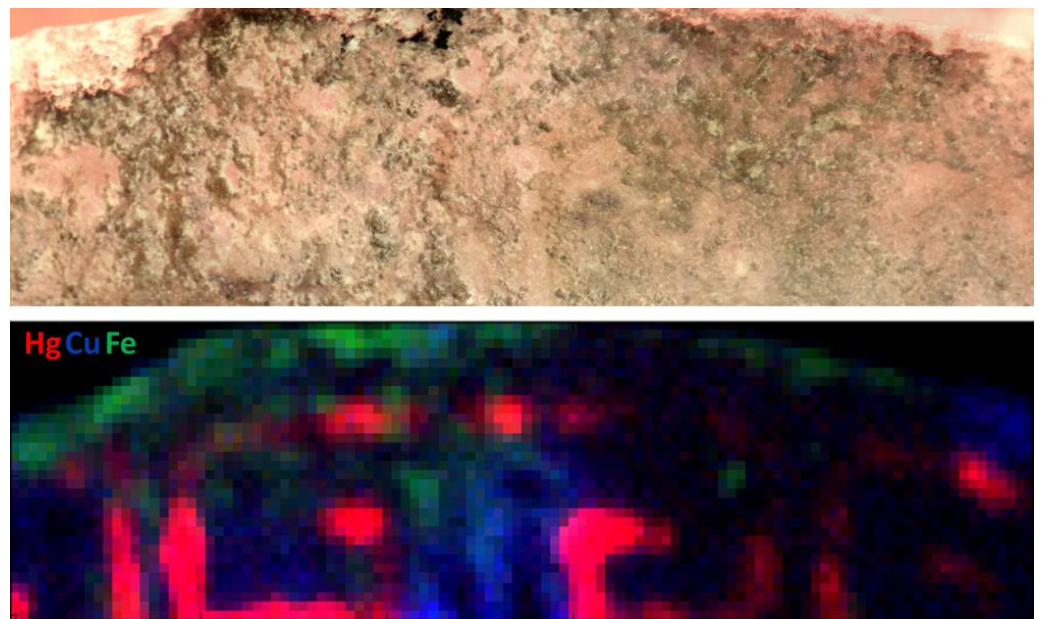


Figure 5. Composite elemental maps of Cu, Hg, and Fe resulting from scanning the diadem (area B of Figure 4), whose decoration hides underneath a thick accretion (top image).

Two areas of the proper right wing (Figure 4, areas A and E) were also scanned with sXRF to reconstruct the design and color scheme of the feathers, even where minimal residues of the original pigments were observed. The detection of Hg indicates that cinnabar was used for the red feathers, while Cu indicates the use of two Cu-containing pigments for the blue feathers (Figure 6).



Figure 6. Composite elemental maps of Cu, Fe, and Hg showing the distribution of the corresponding pigments (Cu for azurite and Egyptian blue; Hg for cinnabar) on the wing (area A of Figure 4). (left), VIS image of the scanned area; (middle), stacked VIS-VIL image; (right), XRF map.

The combination of sXRF and VIL revealed the original design of alternating red (Hg, cinnabar) and blue (Cu, azurite, as discussed later) feathers outlined by black lines, against a possibly lighter blue background (Cu, Egyptian blue). The distribution of Egyptian blue and azurite was reconstructed by layering the elemental map of Cu over the VIL image. Although the distribution of Fe appears denser around some of the flight feathers (Figure 6), the original presence and application of Fe-based pigments in the wing remains speculative and deserves further investigation.

Hg and Cu are also the most significant elements in the scale-shaped design of the breast feathers, revealing a red and blue pattern obtained by painting with cinnabar and azurite, as determined by minimally invasive analysis (Figure 7). A higher concentration of Fe around the chest feathers, also corresponding to lines visible in IRR, suggested that a Fe-based pigment was used to outline the scales.

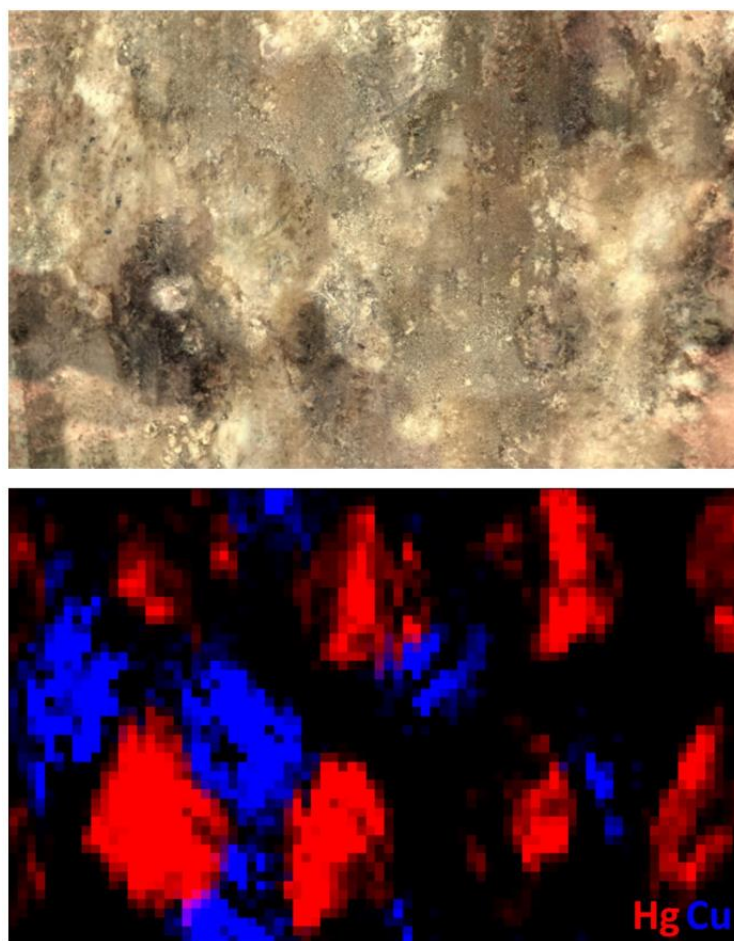


Figure 7. Composite elemental maps of Cu and Hg reconstructing the scale design on the chest of the sphinx (area C of Figure 4). The VIS image at the top shows how altered this area is.

Scanning XRF failed to map the pigment distribution on the capital, most likely because the pigment remains were too slight to be detected by this technique. Incised lines, as well as the faint image of the central rosette in relief, which resulted from differential weathering, can be seen on the plinth at the top of the left side of the capital. This mirrors the visible remains of color that can be seen on the right side by the naked eye.

Point XRF analysis of the stele affirmed the use of Fe-based pigments, most likely ochres, for the red of the background and the hair of the youth. Analysis of the aryballos identified the presence of lines of darkened red containing Hg and S, most likely cinnabar, Cu-based blue without VIL luminescence in a crevice of the neck, most likely azurite, and possibly Fe-containing yellow pigment remains.

3.2. Minimally Invasive Analysis of Pigments

According to the data acquired by non-invasive analyses, the sculpture's palette included two reds, two blues, black, possibly yellow and white. In order to collect further and complementary information about these pigments, and, when possible, to rule out the existence of pigment mixtures and preparation layers, ten micro-samples were collected from representative areas of the sphinx surface and analyzed by a combination of SEM-EDS, μ Raman, and μ XRD analysis. The collected samples are listed in Table 1 and their sampling locations are reported in Figure 4, while results are presented for each color group in the following sections.

Table 1. List of micro-samples removed from the sphinx, with corresponding description and sampling locations.

Sample	Description	Color	Location
S1B	Loose particle	Blue	End of the tail
S2R	Loose particles	Red	Flight feather of the proper right wing
S3R	Loose particles	Brown/Red	Lioness skin, between wings
S4R	Cross section	Red	Sphinx's hair
S5R	Loose particles	Brown/Red	Front left leg
S6Y	Loose particles	Yellow	Back of the diadem
S7Bl	Loose particles	Black	Flight feather outline of the proper right wing
S8Bl	Loose particles	Black	Genitals of the sphinx
S9W	Loose particles	White	Left eye of the sphinx
S10R	Cross section	Red	Sphinx's hair

3.2.1. Blue Pigments

If the combination of VIL and sXRF provided information about the presence and distribution of Egyptian blue, the identification of the second Cu-based blue required further analysis. The second Cu-based blue was found in areas of the youth's aryballos, the sphinx's chest, the wing feathers, the diadem, and the end of the tail. Observation of loose pigment particles collected from the end of the sphinx's tail (sample 1B, Table 1) displayed a bright blue color under PLM, typical of azurite (Figure 8), although sparse greenish-blue grains, most likely weathered azurite, were also identified in the mixtures. When imaged by SEM, the particles were rather angular in shape and their size ranged from a few microns to about 100 μ m (Figure 8). Fine-grained gypsum particles were present on the azurite particles and dispersed in the loose sample. The abundance and distribution of gypsum particles in the sample might be indicative of an intentional addition to the paint mixture, although a secondary deposition cannot be ruled out. Other accessory phases were calcite and fine-grained silicates, mainly quartz and feldspars, rare iron oxides/hydroxides, and chromite. The conclusive identification of azurite in this sample was achieved by Raman spectroscopy and the characteristic Raman bands of this mineral pigment at 250, 401, 545, 765, 835, 940, 1095, 1420, and 1578 cm^{-1} (Figure 8).

3.2.2. Red Pigments

The presence of cinnabar as deduced from non-invasive XRF analysis was confirmed by Raman (252, 282, and 343 cm^{-1}), μ XRD, and SEM-EDS analyses of a few pigment particles collected from a flight feather (sample 2R).

Bright red particles of pigment, consistent with this interpretation, were imaged in these locations by digital microscopy, surrounded by darker particles of weathered cinnabar, most likely metacinnabar. The presence of cinnabar was detected in the youth's aryballos and the sphinx's chest, wing, diadem, necklace, and eyes. No traces of gypsum were detected by Raman, μ XRD, or SEM-EDS, suggesting that cinnabar was not mixed in with gypsum.

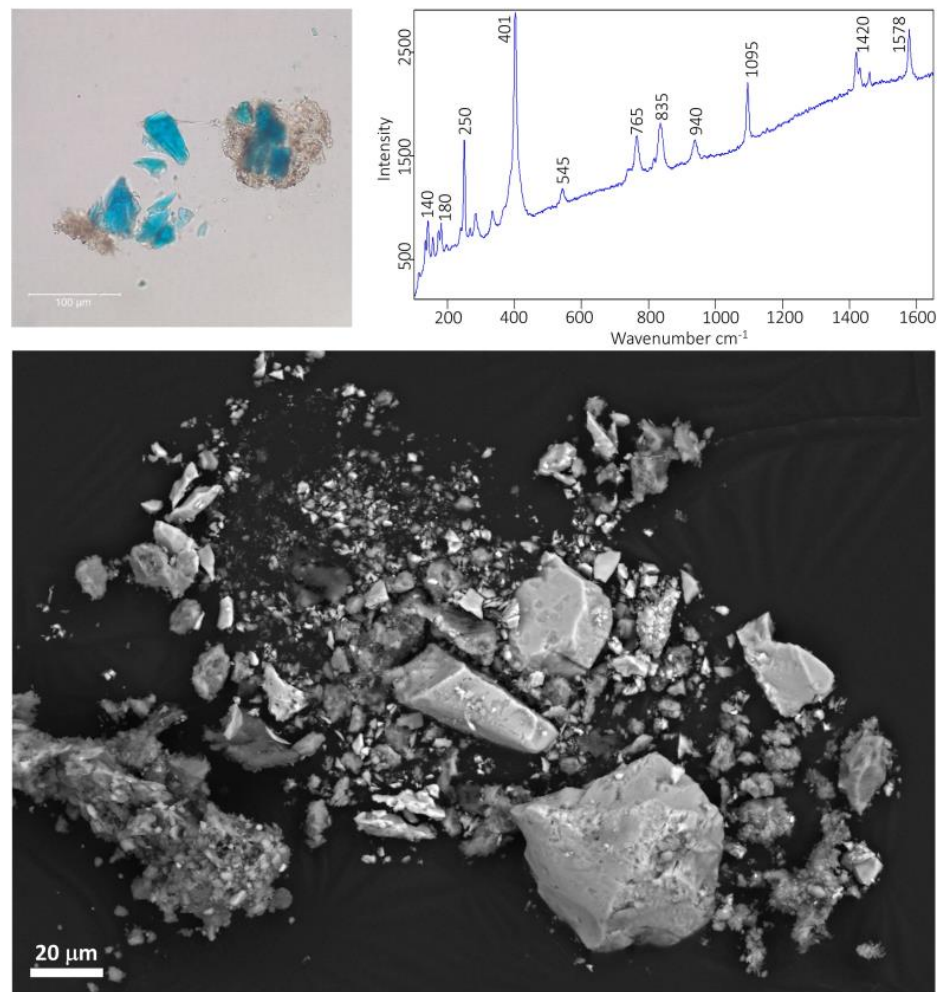


Figure 8. BSE image of sample 1B showing particles shapes and grainsize (**bottom**); PLM image of sample 1B (**top left**) and Raman spectrum measured on one of the blue particles (**top right**).

Two cross sections from the sphinx's hair (samples S4R and S10R), where Fe-containing pigments were identified by non-invasive XRF, show a complete stratigraphy that included the marble substrate, a red pigment layer, and a thick accretion. The stratigraphy indicated that the pigment was applied directly to the marble surface without a preparation layer, confirming the observations collected by digital microscopy (Figure 9). The pigment layer consisted of clusters of very fine Fe-oxide platelets not exceeding 1 μm in size, associated with very fine silicates, most likely clay minerals, rare quartz, and very rare pyrite, suggesting that this red pigment was a highly refined red ochre. The presence of hematite was identified by Raman spectroscopy and μXRD. It is worth noticing that traces of arsenic (As) were detected in hematite particles (up to 1 wt%) by EDS analysis, an occurrence reported in red lumps of pigments excavated from the pigment workshop of the Koan agora, Kos, Greece [38].

Scattered clusters of platy Fe-oxide/hydroxide particles, most likely hematite, containing traces of As, and fine-grained silicates, were also identified in a loose sample collected from the lioness skin between the wings (sample 3R, Figure 10), suggesting that red ochre was used for the decoration of this portion of the sphinx's body. Given the nature of the sample, it was not possible to determine if red ochre was used in purity or mixed in with other pigments.

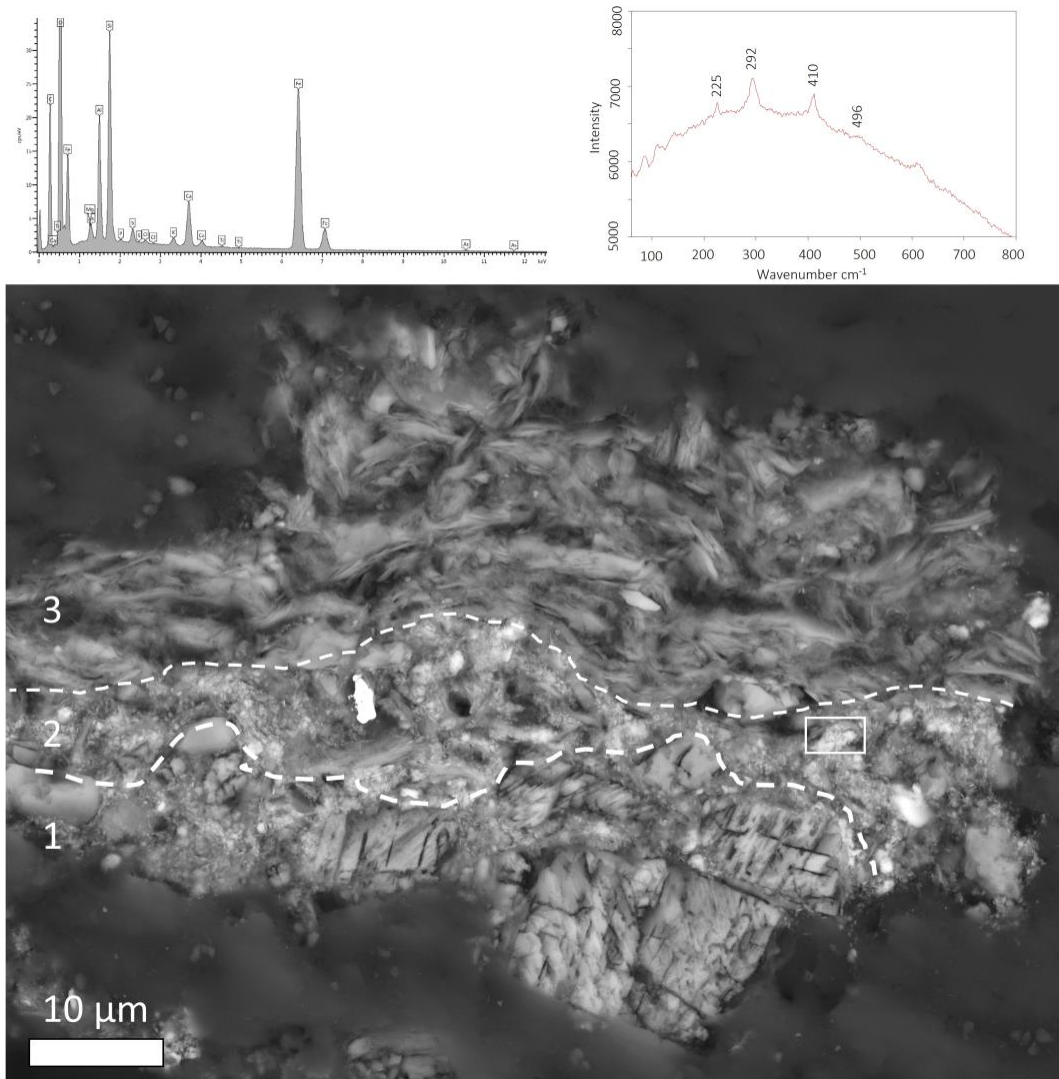


Figure 9. BSE image of cross section 4R (**bottom**) showing the paint stratigraphy of the hair (1. Marble substrate; 2. Paint layer; 3. Accretion); EDS spectrum (**top left**) of a sporadic cinnabar particle in the paint layer (very bright particle at the center of layer 2); Raman spectrum of the hematite particle indicated in the figure (**top right**).

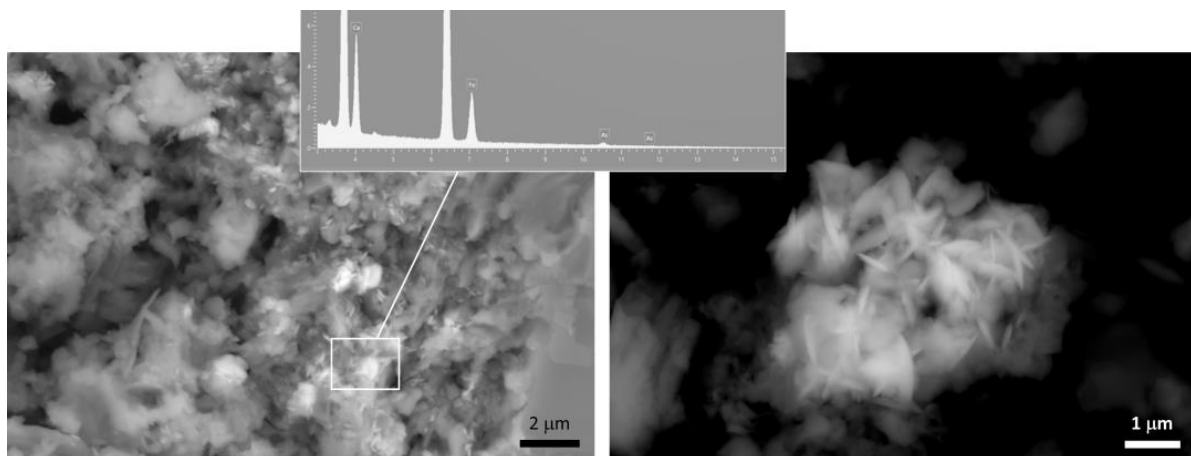


Figure 10. BSE images of sample 3R with corresponding EDS spectrum (**left**), and of a typical platy Fe-oxide/hydroxide particle (**right**).

A few particles of cinnabar were detected in cross section S4R from the sphinx's hair (Figure 9) and from a loose sample collected from the front left leg (sample 5R). Although sparse cinnabar particles could be the result of both an intentional addition and a contamination of the artist's tools, their recurrent presence associated with ochres suggest that cinnabar was intentionally added to modify the hue of these pigments.

Similarly, traces of Ca and S were detected by EDS analysis of the sphinx's hair and wings, and gypsum was identified in ochre samples by μ XRD, suggesting that fine-grained gypsum was likely intentionally added to the ochre layers. However, the analysis could not exclude the possibility that the presence of gypsum was the result of a secondary deposition that took place during the burial of the sculpture.

3.2.3. Yellow Pigments

The identification and characterization of yellow pigments on the sphinx was challenging, and, for the most part, inconclusive. The main difficulties arose from the fact that, despite the presence of a visible yellowish patina on areas such as the lioness's body and the sphinx's face, or in areas surrounding the feathers, very little original pigment remains, and that what remains is often highly contaminated. One micro-sample consisting of loose particles of yellow color (sample 6Y) was successfully removed from behind the diadem, where a rather homogeneous yellow layer is still visible. Raman spectroscopy and SEM-EDS analysis revealed the presence of hematite and goethite, associated with very fine-grained alumino-silicates and traces of lead oxides and gypsum. This association of hematite, goethite, and clay minerals was interpreted as a pigment, which is consistent with a yellow ochre. In support of this interpretation was the finding of few particles of lead oxide, a compound that has been reported in red ochres excavated from the pigment production site of Kos [38]. No traces of arsenic-containing yellow pigments were detected, ruling out the use of orpiment, which was frequently chosen by artists in ancient times [39].

3.2.4. Black Pigments

Black color is visible in the wings, outlining the flight feathers, separating areas painted with azurite and Egyptian blue, in the left eyebrow, and highlighting the sphinx's genitals.

Raman analysis of two samples, one from the flight feathers and one from the sphinx's genitals (samples 7Bl and 8Bl, respectively), allowed detection of the typical broad bands of amorphous carbon-based black pigments at ~ 1335 and ~ 1585 cm^{-1} . SEM observations showed that this black pigment consisted of small particles not exceeding 5 μm in size, with irregular and variable shapes. None of the particles showed morphologies clearly associated with chars, such as typical cellular structures of wood or vine blacks. Although the lack of phosphorus in the EDS analysis of these particles allowed us to rule out the use of bone/ivory black, the exact typology of this carbon-based black remains undetermined, even though the use of lampblack might be hypothesized by exclusion.

3.2.5. White Pigments

Only minimal vestiges of white areas are visible in a small portion of the left eye of the sphinx. A few particles were collected from this area (sample 9W) and analyzed by Raman, μ XRD, and SEM-EDS. Results indicated that these white, loose particles consisted predominantly of fine, angular calcite particles, while no traces of other common white pigments, such as lead white, kaolin, or gypsum, were identified. Given that the sampled area shows signs of mechanical removal of burial accretion, possibly attempted to reveal the colored iris, it is likely that the sampled calcite particles originate from the abraded marble substrate, rather than being an intentionally applied pigment.

4. Conclusions

The exhibition *Chroma: Ancient Sculpture in Color* was used as an occasion to obtain novel information on the polychromy of an Attic Archaic funerary stele by using a combination of non-invasive and minimally invasive techniques. To date, only a few in-depth

studies on Greek Archaic sphinxes have been published [15,39], and the number decreases if we restrict the focus on funerary sphinxes. Thus, the comprehensive study offered by this paper contributes to filling a gap currently present in the literature.

Despite limited accessibility to the sphinx, the early combination of in-situ multiband imaging and sXRF allowed for the identification of extant pigments and their distribution, and was essential in guiding the removal of micro-samples.

The investigation revealed a color palette that includes red and yellow ochres, cinnabar, azurite, Egyptian blue, and carbon-based black. This color palette is consistent with that employed in contemporary late 6th century BCE polychrome artworks [40,41].

The pigments were applied directly to the marble substrate. Egyptian blue was used between the flight feathers of the wings, probably to simulate the sky, whereas azurite and cinnabar were abundantly used to render the flight and breast feathers, to realize the meandering pattern of the diadem, and to decorate fine details on the shaft, such as the aryballos. A fine-grained red ochre, rich in hematite, was used for the decoration of the hair and the shaft background. More problematic is understanding how and where yellow ochres were used on the sculpture. If this pigment was unambiguously identified in the back of the crown and other locations, such as in the crown's background, the leonine body, and around the flight and breast feathers, its presence can only be postulated by combining information collected by digital microscopy, multiband imaging, and XRF analysis.

Most likely, various typologies of pigments, containing different types and relative ratios of Fe-oxides and hydroxides, cinnabar, and possibly gypsum, were used in different parts of the stele, the capital, and the sphinx finial, including both the face and leonine body. Currently, only the red used for the sphinx was properly characterized, while the other Fe-based pigment assemblages remain undetermined until further analysis. Similarly undetermined is the presence of Pb-based pigments, such as cerussite. While characteristic Pb X-ray lines are present in several XRF spectra collected from the funerary stele, no Pb-containing compounds were positively identified during this investigation.

Overall, the identification of the color palette used on the sculpture may contribute to a better understanding of the use and meaning of colors in funerary monuments dating to the Archaic period, and their communicating aesthetics. The scientific results highlighted in the *Chroma* exhibition were crucial in informing the reconstruction of the intricate polychromy of the sphinx, eventually displayed next to the original sculpture. Scientific results were featured in the exhibition narrative and incorporated into an augmented reality experience, allowing visitors to elevate their observation and understanding of the artwork with an increased level of engagement.

Supplementary Materials: The following supporting information can be downloaded at <https://www.mdpi.com/article/10.3390/app13053102/s1>: Figure S1: Mobile dark room; Figure S2: UV light image of the sphinx; Figure S3: UV-VIS stacked image; Figure S4: Micrographs of color remains; Figure S5: XRF line scan of the sphinx's eye; Figure S6: Detail of the sphinx's diadem.

Author Contributions: Conceptualization, F.C. and E.B.; methodology, F.C. and D.H.A.; formal analysis, F.C., E.B. and D.H.A.; investigation, F.C., E.B. and D.H.A.; resources, F.C., E.B. and D.H.A.; data curation, F.C., E.B. and D.H.A.; writing—original draft preparation, E.B.; writing—review and editing, F.C. and D.H.A.; visualization, F.C., E.B. and D.H.A.; supervision, F.C. All authors have read and agreed to the published version of the manuscript.

Funding: This research received no external funding.

Institutional Review Board Statement: Not applicable.

Informed Consent Statement: Not applicable.

Data Availability Statement: Not applicable.

Acknowledgments: The authors are indebted to Seán Hemingway and Sarah Lepinski, The Met Department of Greek and Roman, curators of the *Chroma* exhibition. The authors would like to acknowledge Marco Leona, The Met Department of Scientific Research, for the generous support, as well as Lisa Piloni, The Met Department of Objects Conservation. We owe special gratitude to Vinzenz Brinkmann and Ulriche Koch-Brinkmann for the fruitful discussions during the whole project.

Conflicts of Interest: The authors declare no conflict of interest.

References

- Vlassopoulou, C. History of the research on polychromy in sculpture. In *Archaic Colors*; Acropolis Museum: Athens, Greece, 2012.
- Panagiotidou, D.; Merkouri, E.; Kokkinou, L. The use of color in Archaic sculpture. In *Archaic Colors*; Acropolis Museum: Athens, Greece, 2012.
- Gasanova, S.; Pagès-Camagna, S.; Andriotti, M.; Lemasson, Q.; Brunel, L.; Doublet, C.; Hermon, S. Polychromy analysis on Cypriot archaic statues by non- and micro-invasive analytical techniques. *Archaeometry* **2017**, *3*, 528–546. [[CrossRef](#)]
- Østergaard, J.S.; Schwartz, A. A Late Archaic/Early Classical Greek Relief with Two Hoplites (Ny Carlsberg Glyptotek IN 2787). *Jahrb. Des Dtsch. Archäologischen Inst.* **2022**, *137*, 1–37.
- Ike, K. The polychromy of the Parthenon: A reconstruction study on its meaning and system. *J. Archit. Plann. Environ. Eng. All* **2000**, *537*, 265–273. [[CrossRef](#)] [[PubMed](#)]
- Aggelakopoulou, E.; Sotiropoulou, S.; Karagiannis, G. Architectural Polychromy on the Athenian Acropolis: An In Situ Non-Invasive Analytical Investigation of the Colour Remains. *Heritage* **2022**, *5*, 756–787. [[CrossRef](#)]
- Kefalidou, E. Late Archaic polychrome pottery from Aiani. *Hesperia* **2001**, *70*, 183–219. [[CrossRef](#)]
- Bourgeois, B.; Jeammet, V. The polychromy of Greek terracotta figurines: Material approach to a pictural culture. *Rev. Archéol.* **2020**, *69*, 3–28. [[CrossRef](#)]
- Bertram, H. Chapter Five: The Archaic and Classical Figurines. *Mouseion* **2021**, *18*, 134–162. [[CrossRef](#)]
- Kiilerich, B. Towards a ‘Polychrome History’ of Greek and Roman Sculpture. *J. Art. Hist.* **2016**, *15*, 1.
- Panzanelli, R.; Schmidt, E.D.; Lapatin, K. *The Color of Life: Polychromy in Sculpture from Antiquity to the Present*; Getty Publications: Los Angeles, CA, USA, 2008.
- Brinkmann, V.; Primavesi, O.; Hollein, M. *Circumlitio. The Polychromy of Antique and Medieval Sculpture*; Hirmer Publishers: Munich, Germany, 2010.
- Brinkmann, V.; Dreyfus, R. *Gods in Color: Polychromy in the Ancient World*; DelMonico/Prestel: Munich, Germany, 2017.
- Pandermalis, D. *Archaic Colors*; Argo Printing House: Athens, Greece, 2012.
- Gasanova, S.; Pagès-Camagna, S.; Andriotti, M.; Hermon, S. Non-destructive in situ analysis of polychromy on ancient Cypriot sculptures. *Archaeol. Anthropol. Sci.* **2018**, *10*, 83–95. [[CrossRef](#)]
- Karydas, A.G.; Brecolouaki, H.; Bourgeois, B.; Jockey, P.; Zarkadas, C. In-situ XRF Analysis of raw pigments and traces of polychromy on marble sculpture surfaces. Possibilities and limitations. In Proceedings of the 28th International Symposium on the Conservation and Restoration of Cultural Property: Non Destructive Examination of Cultural Objects-Recent Advances in X-ray Analysis, Tokyo, Japan, 1–3 December 2004.
- Blume, C. The role of the stone in the polychrome treatment of Hellenistic sculptures. In Proceedings of the IX ASMOSIA Conference: Interdisciplinary Studies on Ancient Stone, Tarragona, Spain, 8–13 June 2009.
- Abbe, M.B.; Borromeo, G.E.; Pike, S. A Hellenistic Greek marble statue with ancient polychromy reported to be from Knidos. In Proceedings of the IX ASMOSIA Conference: Interdisciplinary Studies on Ancient Stone, Tarragona, Spain, 8–13 June 2009.
- Campbell, L. Polychromy on the Antonine Wall Distance sculptures: Non-destructive Identification of pigments on Roman reliefs. *Britannia* **2020**, *51*, 175–201. [[CrossRef](#)]
- Verri, G.; Clementi, C.; Comelli, D.; Cather, S.; Piqué, F. Correction of Ultraviolet-Induced Fluorescence Spectra for the Examination of Polychromy. *Appl. Spectrosc.* **2008**, *62*, 1295–1302. [[CrossRef](#)] [[PubMed](#)]
- Stager, J.M.S. *Seeing Color in Classical Art*; Cambridge University Press: Cambridge, UK, 2022.
- Neri, E.; Alfeld, M.; Nasr, N.; de Viguier, L.; Walter, P. Unveiling the paint stratigraphy and technique of Roman African polychrome statues. *Archaeol. Anthropol. Sci.* **2022**, *14*, 118. [[CrossRef](#)]
- Abbe, M. Polychromy. In *The Oxford Handbook of Roman Sculpture*; Friedland, E.A., Grunow Sobocinski, M., Gazda, E.K., Eds.; Oxford University Press: New York, NY, USA, 2015; pp. 173–188.
- Alfeld, M.; Mulliez, M.; Martinez, P.; Cain, K.; Jockey, P.; Walter, P. The Eye of the Medusa: XRF imaging reveals unknown traces of antique polychromy. *Anal. Chem.* **2017**, *89*, 1493–1500. [[CrossRef](#)] [[PubMed](#)]
- Brøns, C.; Stenger, J.; Bredal-Jørgensen, J.; Di Gianvincenzo, F.; Brandt, L.Ø. Palmyrene Polychromy: Investigations of Funerary Portraits from Palmyra in the Collections of the Ny Carlsberg Glyptotek, Copenhagen. *Heritage* **2022**, *5*, 1199–1239. [[CrossRef](#)]
- Odrizola, C.P.; Beltrán Fortes, J.; Loza Azuaga, M.L.; Martínez Blanes, J.M. Polychromy in Roman Portraits from Asido (Medina Sidonia, Cádiz, Spain). Livia, Germanicus and Drusus Minor. *Herit. Sci.* **2022**, *10*, 108. [[CrossRef](#)]
- Abramitis, D.H.; Basso, E.; Carò, F.; Hemingway, S.; Lepinski, S.; Leona, M. Ancient Greek Sculpture in Color. *Perspective* **2022**. Available online: <https://www.metmuseum.org/perspectives/articles/2022/8/new-research-greek-sphinx> (accessed on 22 February 2023).

28. Richter, G.M.A. An Archaic Greek Sphinx. *Metropol. Mus. Art B* **1940**, *35*, 178–180. [[CrossRef](#)]
29. Richter, G.M.A.; Hall, L.F. Polychromy in Greek Sculpture. *Metropol. Mus. Art B* **1944**, *2*, 233–240. [[CrossRef](#)]
30. Hemingway, S.; Lepinski, S.; Abramitis, D.H.; Basso, E.; Carò, F.; Leona, M. New Research on the Polychromy of an Archaic Grave Stele and Finial in the Form of a Sphinx in the Collection of The Metropolitan Museum of Art, New York. In Proceedings of the 10th International Round Table on Polychromy in Ancient Sculpture and Architecture: Color and Space. Interfaces of Ancient Architecture and Sculpture, Berlin, Germany, 10–13 November 2020.
31. Solé, V.A.; Papillon, E.; Cotte, M.; Walter, P.; Susini, J. A multiplatform code for the analysis of energy dispersive X-ray fluorescence spectra. *Spectrochim. Acta B* **2007**, *62*, 63–68.
32. McCormack, J. The darkening of cinnabar in sunlight. *Miner. Depos.* **2000**, *35*, 796–798. [[CrossRef](#)]
33. Terrapon, V.; Béarat, H. A study of cinnabar blackening: New approach and treatment perspective. In Proceedings of the 7th International Conference on Science and Technology in Archaeology and Conservation at Petra, Petra, Jordan, 7–12 December 2010.
34. Elert, K.; Pérez Mendoza, M.; Cardell, C. Direct evidence for metallic mercury causing photo-induced darkening of red cinnabar tempera paints. *Commun. Chem.* **2021**, *4*, 174. [[CrossRef](#)] [[PubMed](#)]
35. Spring, M.; Grout, R. The Blackening of Vermilion: An Analytical Study of the Process in Paintings. *NAACOG Tech. Bull.* **2002**, *23*, 50–61.
36. Keune, K.; Boon, J.J. Analytical imaging studies clarifying the process of the darkening of vermilion in paintings. *Anal. Chem.* **2005**, *77*, 4742–4750. [[CrossRef](#)]
37. Nöller, R. Cinnabar reviewed: Characterization of the red pigment and its reactions. *Stud. Conserv.* **2015**, *60*, 79–87. [[CrossRef](#)]
38. Kostomitsopoulou Marketou, A.; Kouzeli, K.; Facorellis, Y. Colourful earth: Iron-containing pigments from the Hellenistic pigment production site of the ancient agora of Kos (Greece). *J. Archaeol. Sci. Rep.* **2019**, *26*, 101843. [[CrossRef](#)]
39. Sargent, M.L.; Spaabek, L.R.; Scharff, M.; Østergaard, J.S. Documentation and investigation of traces of colour on the Archaic Sphinx NCG IN 1203. In *Tracking Colour. The Polychromy of Greek and Roman Sculpture in the Ny Carlsberg Glyptotek, Preliminary Report 1*; Østergaard, J.S., Copenhagen Polychromy Network, Eds.; Ny Carlsberg Glyptotek: Copenhagen, Denmark, 2009; pp. 74–89.
40. Brecolaki, H. “Precious colours” in Ancient Greek polychromy and painting: Material aspects and symbolic values. *Revue. Archéol.* **2014**, *1*, 3–35. [[CrossRef](#)]
41. Katsaros, T. Pigments—Composition and Origin. In *Archaic Colors*; Acropolis Museum: Athens, Greece, 2012; pp. 18–24.

Disclaimer/Publisher’s Note: The statements, opinions and data contained in all publications are solely those of the individual author(s) and contributor(s) and not of MDPI and/or the editor(s). MDPI and/or the editor(s) disclaim responsibility for any injury to people or property resulting from any ideas, methods, instructions or products referred to in the content.